CRYSTALLIZATION KINETICS OF GLASS-CERAMICS BY DIFFERENTIAL THERMAL ANALYSIS

M. GHASEMZADEH, A. NEMATI*, A. NOZAD**, Z. HAMNABARD** AND S. BAGHSHAHI***

Deptartment of Materials Eng., Science & Research Branch,
Islamic Azad University, Tehran, Iran
**Dept. of Materials Sci. & Eng., Sharif University of Technology, Tehran, Iran*
***Ceramic Group, Material Research School, Karaj, Iran*
****Faculty of Engineering, Imam Khomeini International University, Qazvin, Iran*

E-mail: ghasemzadeh@kiau.ac.ir

Submitted November 11, 2010; accepted May 11, 2011

Keywords: Crystallization kinetics; Activation energies; Glass ceramics; Microstructure; Phlogopite

The crystallization behavior of fluorphlogopite, a glass-ceramic in the MgO–SiO_2–Al_2O_3–K_2O–B_2O_3–F system, was studied by substitution of Li_2O for K_2O in the glass composition. DTA, XRD and SEM were used for the study of crystallization behavior, formed phases and microstructure of the resulting glass-ceramics. Crystallization kinetics of the glass was investigated under non-isothermal conditions, using the formal theory of transformations for heterogeneous nucleation. The crystallization results were analyzed, and both the activation energy of crystallization process as well as the crystallization mechanism were characterized. Calculated kinetic parameters indicated that the appropriate crystallization mechanism was bulk crystallization for base glass and the sample with addition of Li_2O. Non-isothermal DTA experiments showed that the crystallization activation energies of base glasses was in the range of 234-246 KJ/mol and in the samples with addition of Li2O was changed to the range of 317-322 KJ/mol.

INTRODUCTION

The fabrication technology of glass-ceramics, the glass composition, the nature of the nucleating agent and the thermal history, all greatly affect the microstructure and properties of these materials [1]. Mica glass-ceramics are well known as typical machinable ceramics and have already found several applications as engineering materials [2-5]. In the ternary Li_2O–K_2O–SiO_2 system, high mobility of lithium ions cause the formation of eutectics with low melting point. Therefore Li_2O is a suitable oxide to increase the rate of melting and facilitates the crystallization. Several investigations have been carried on the influence of different additives on the crystallization behavior and type of precipitated phases in the machinable glass-ceramics [6-8]. Henry and Hill [4] have investigated the influence of substituting lithia for magnesia on the nucleation and crystallization behaviour of SiO_2 Al_2O_3 MgO/ Li_2O MgF_2BaO/K_2O glasses and investigated the microstructural development, mechanical properties and machinability of the resulting glass-ceramics. According to their results substituting lithia for magnesia rduced the glass transition temperature, whilst the thermal expansion coefficient increased with increasing lithia and potassia content. They have found that the activation energies for crystallization did not change significantly with lithia content. Trauta et al.[9] prepared transparent lithium-mica glass-ceramics and investigated influence of MgF_2 as nucleating agent for crystallization in this system. They showed precipitation of very fine mica crystals in a continuous glass are spinodal phase separation made the microstructure finer. Consequently, the heated specimens showed higher transmittance to visible light and became colorless. Due to the mica crystals formation, which were precipitated in the glass phase, the specimens showed the machinability characteristic, as well [9-11].

DTA is a powerful tool in studying the crystallization kinetics of glass [12-13]. Two methods, namely isothermal and non-isothermal methods, are used for the differential thermal analysis of glass samples. Johnson-Mehl-Avrami (JMA) equation is generally used for the kinetic analyses of isothermal DTA data. In the JMA method, glass samples are quickly heated and soaked at a temperature above the glass transition temperature. In this case, crystallization occurs at a fixed temperature. Nonetheless, in non-isothermal method, glass samples are heated at a certain heating rate and crystallized during the thermal analysis scan [13]. The non-isothermal method is more simple and quicker than the isothermal one.

Activation energy and crystallization mechanisms are the most important kinetic parameters for the crystallization of glasses. These parameters can be obtained by experimental DTA results using proper equations proposed to interpret non-isothermal data [14,15]. However, most of these equations assume that the variation of peak crystallization temperature is directly related to the heating rate [14-16]. These equations and assumption help us to understand the nature of the crystallization mechanisms in different glass forming systems.

In this study, the influence of substitution of Lithia for potassia on the crystallization and microstructure of mica glass-ceramic were investigated. Kissinger [15], Matusita and Sakka [14] and Ozawa [16] equations were used to determine the crystallization mechanism and the activation energy values for crystallization.

THEORETICAL

In this paper, the kinetic parameters of the glass-crystallization were determined under non-isothermal conditions applying three different equations, Kissinger [15], Matusita and sakka [14]and ozawa [16]. In these equations it was assumed that the variation of peak crystallization temperature, T_p, is directly related to the heating rate, α. For example, in the Kissinger method, the crystallization peak temperature is monitored as a function of the heating rate and the following relationship is applied:

$$\ln(\alpha/T_p^2) = (-E_{ck}/RT_p) + \text{Constant.} \qquad (1)$$

where E_{ck} is the activation energy for crystallization, determined by the Kissinger method. A plot of $\ln(\alpha/T_p^2)$ vs. $1/T_p$ should be a straight line, from which the slope can be determined (E_{ck}). Matusita and Sakka [14] stated that Equation (1) is valid only when crystal growth occurs on a fixed number of nuclei. Incorrect values for the activation energy are obtained if a majority of the nuclei are formed during the DTA measurement, due to the number of nuclei continuously varying with α. They have proposed a modified form of the Kissinger equation as given below:

$$\ln(\alpha^n/T_p^2) = (-mE_c/RT_p) + \text{Constant.} \qquad (2)$$

where E_c is the modifed activation energy for crystallization and m is the numerical factor which depends on the dimensionality of crystal growth. When surface crystallization predominates, $m = 1$ and when the bulk crystallization is predominanted, $m = 3$ (as shown in Table 2) [13]. In different mechanism the value of m and n is related. For example $m = n$, when crystallization at different heating rates occurs on a fixed number of nuclei (i.e. the number of nuclei is constant during DTA runs at different values of α) or $m = n - 1$; when nucleation occurs during DTA and the number of nuclei in the glass is inversely proportional to α. In addition, when surface crystallization predominates, $m = n = 1$ and Equation (2) essentially reduces to the Kissinger equation in which E_{ck} becomes equals to E_c.

In the case of bulk crystallization, E_{ck} does not necessarily equals to E_c. Rather, a close inspection of Equations (1) and (2) shows that, the following relation might be applied:

$$E_c = (n/m)\, E_{ck} - 2((n-1)/m)RT_p \qquad (3)$$

For most oxide glass systems, $E_c \geq 20\ RT_P$ [13] and therefore, the elimination of $2[(n-1)/m]RT_p \leq 2\ RT_p$ in Equation (2) will result in an error less than only 10% in the value of E_c. This error is within the error range of the DTA measurements. Then one can obtain the following relation:

$$E_c\ (n/m)E_{ck} \qquad (4)$$

For the case of $m = n$, i.e. , when crystallization occurs on a fixed number of nuclei, $E_{ck} = E_c$. Thus, for predominantly surface crystallization or for crystal growth that occurs in a fixed number of nuclei, the analysis of DTA data by the Kissinger model (Equation (1)) yields the correct value of E_c. When the number of nuclei changes during the DTA measurements, either, Equation (2) should be used or E_{ck} determined from Equation (1) should be multiplied by the term (n/m) to obtain the correct activation energy.

Form the exothermic peak, the Arrami parameter, n, can be obtained by using the following modified Ozawa equation [16]:

$$\left(\frac{d\{\ln[-\ln(1 - x)]\}}{dIn\alpha}\right)_T = -n \qquad (5)$$

where x is the volume fraction of crystallized phase at a fixed temperature T at a heating rate of a. Thus, x is the ratio of the partial area at a certain temperature to the total area of a crystallization exotherm.

EXPERIMENTAL

Preparation of glass-ceramics

The chemical composition of base glass (A_0) is presented in Table 1. Two more specimens containing 3.78 and 5.67 wt.% of Li_2O substituted for K_2O in the glass composition were prepared and thereupon named as A_3 and A_5, respectively. The mixtures melted in alumina crucibles at 1450°C in an electric kiln for 2 h. The glass melt was poured in preheated steal moulds and

Table 1. Chemical composition of A_0 specimen (wt.%).

	SiO_2	Al_2O_3	B_2O_3	MgO	K_2O	F	TiO_2	Li_2O
A0	37.96	15.36	6.32	18.1	7.56	9	5.6	0

resulted bulks were annealed at 500°C to eliminate stress. Heat- treatment of the glass blocks were done in a tube electrical furnace at the peak crystallization temperatures with a heating rate of 10°C/min.

Characterization of samples:

The samples were characterized by differential thermal analysis (DTA) using DSC-1500 Rheometric Scientific USA. The reference sample for all compositions was α-Al_2O_3. The crystalline formed phases were detected by X-ray diffraction (Philips PW 1800 X-ray diffractometer). Silicon powder were used as the internal standard material for semi-quantitative measurements. The microstructure of polished and etched specimens (immersion in 10 wt.% HF solution for 20-60s) were observed by scanning electron microscopy Philips XL Seies (XL30). The machinability was evaluated after drilling using a 2mm conventional drill in a drilling force of 30 kN at 300 rpm.

RESULTS AND DISCUSSION

The DTA graphs of the investigated glasses are shown in Figures 1 and 2. Figure 1 showed that the glass transition temperature, "T_g" is 634°C for base glass A_0. This temperature was reduced to 580°C after addition of Li_2O, as shown in the sample A_5. The data indicated that both, T_g and T_p, were decreased with addition of Li_2O in comparison with Li_2O free sample A_0. This is related to Li^+ ions modifying and weakening the network and leading to the reduction of both melting and crystallization onset temperatures as similar results is reported earliear [4]. The presence of Li_2O was found to greatly enhance the crystallizability of the glass. This is obvious from the DTA curves (Figure 1), where the intensity of exothermic crystallization peaks was increased and, at the same time, displaced to lower temperatures. A study carried by J. Henry et al.[4] showed that the activation energy of crystallization decreases in the lithia content compositions. They concluded that substitution of lithia for magnesia improved disruption of glass network and lowered the activation energy for crystallization.

Figure 2 shows the DTA thermogram of A_0 and A_5 samples at the heating rate of 5, 10, 15, 20°C/min. It is observed from this figure that peak crystallization temperature increases with heating rate. The crystallization exotherm curves for the DTA scan at α = 10°C/min are shown in Figure 3. Figure 4 shows the crystallized fraction, x, at a given temperature, is given by $x = A_T/A$,

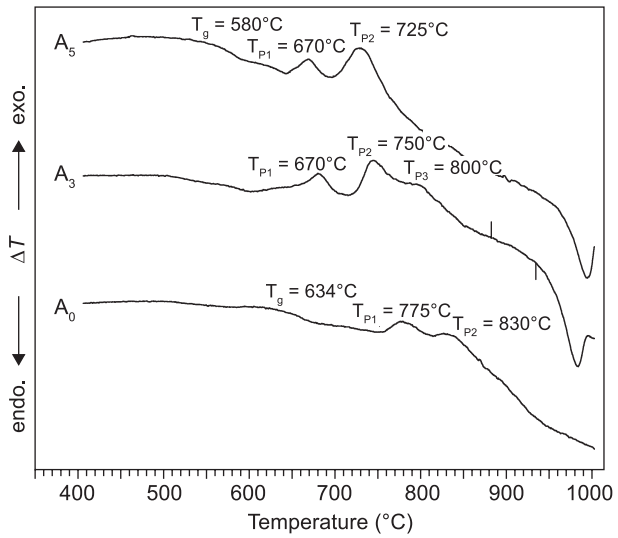

Figure 1. DTA Patterns of the samples (A_0, A_3, A_5).

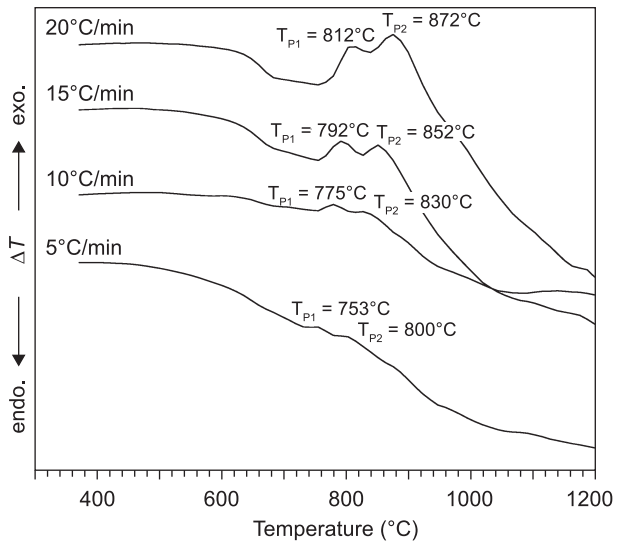

a)

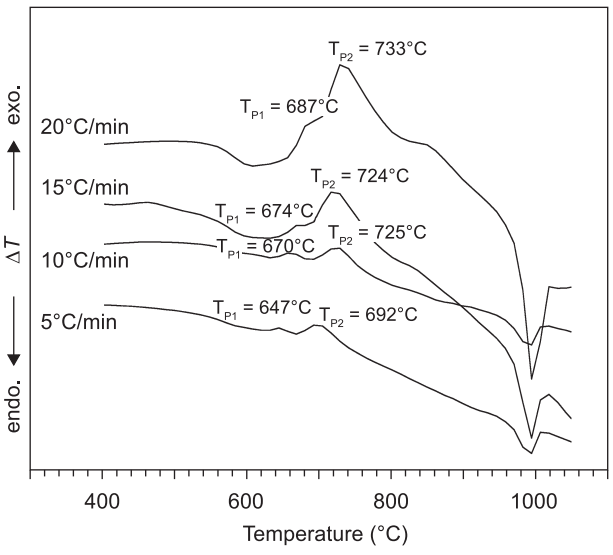

b)

Figure 2. DTA Patterns of the samples for different heating rates: a) A_0, b) A_5.

where A is the total area of the exothermic between the temperature, T_i, where crystallization just begins and the temperature, T_f, where the crystallization is completed, and A_T is the area between T_i and T_f [12]. The graphical representation of the crystallized volume fraction for the exothermic curve shows the typical sigmoid curve as a function of temperature.

Assuming that the nucleation and growth processes had occurred simultaneously in as-quenched samples during the DTA measurements, the data for as-quenched glasses were analyzed by Matusita-Sakka model (Equation (2)) to determine the value of E_c. Since Equation (2) includes the parameters of n and m, their values are first determined using Ozawa model (Equation (5)). Plots of ln (-ln(1-x)) vs. lna for A_0 and A_5 samples are shown in Figure 5, from which the values of n was determined from the slops of these plots the values of *n* found to be 3.17 for A_0 and 1.55 for A_5. These values indicate that bulk crystallizations were dominant in A_0 and A_5 samples. The m value for the A_0 and A_5 should be equal to n-1, i.e 2.17 and 0.55 from Table 2. The values of m = 2.17 and m = 0.55 imply two- and one-dimensional growth, respectively.

By substituting the appropriate values of n, m and *R* (*R* = 8. 3144 J/molk) in Matusita– Sakka equation (Equation (2)), Figure 6 can be obtained for both A_0 and A_5 samples. From the slopes of ln (a^n/T_p^2) vs. $1/T_p$ plots the E_c values are obtained which were 246 KJ/mol for A_0 and 322 KJ/mol for A_5 glasses. Also using the Kissinger model (Equation (1)), E_{ck} values of as-quenched glasses

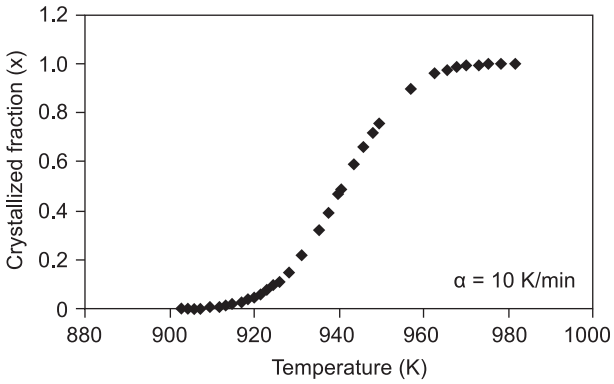

Figure 4. Crystallized fraction as a function of temperature for A_5.

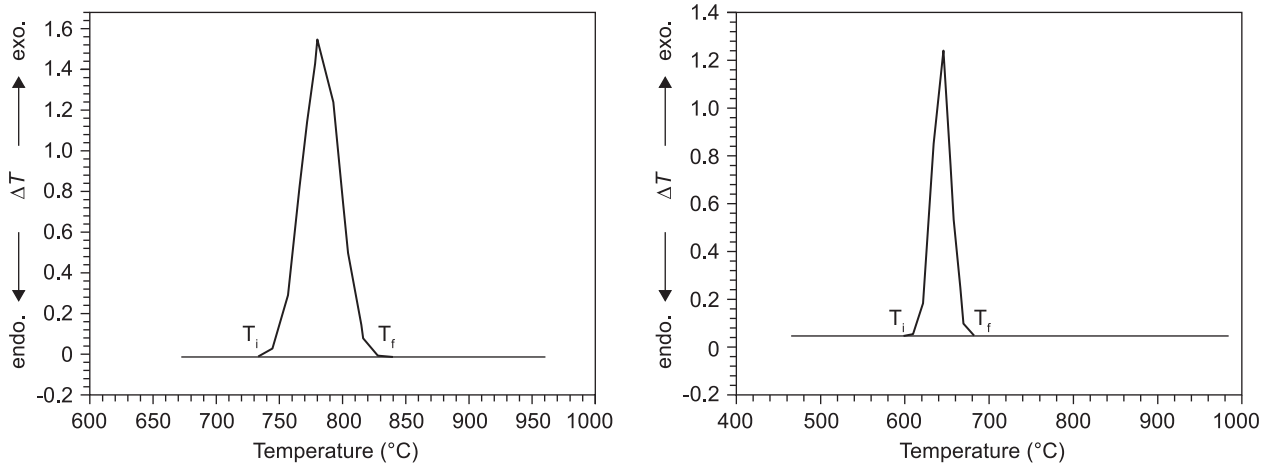

Figure 3. Crystallization curve obtained from DTA (α = 10 K/min) showing area A_T between T_i and T_f for: a) A_0, b) A_5.

Table 2. Values of *n* and *m* for different crystallization mechanisms in heating process [13].

Crystallization mechanism	n	m
Bulk crystallization with a constant Number of nuclei (i.e.the number of nuclei is independent of the heating rate)	–	–
Three-dimensional growth of crystals	3	3
Two-dimensional growth of crystals	2	2
One-dimensional growth of crystals	1	1
Bulk crystallization with an increasing Number of nuclei (i.e. the number of nuclei is inversely proportional to the heating rate)	–	–
Three-dimensional growth of crystals	4	3
Two-dimensional growth of crystals	3	2
One-dimensional growth of crystal	2	1
Surface crystallization	1	1

can be determined from the slope of the plots ln (a/T_p^2) vs. $1/T_p$ (Figure 7). For A_5, E_{ck} is equal to 317 KJ/mol which is close to E_c value determined by Matusita–Sakka model. For A_0, E_{ck} value is equal to 234 KJ/mol which is close to E_c value determined from the Matusita–Sakka model. Substitution of Li_2O for K_2O in the glass composition will move the glass composition further fiom the stoichiometry of the fluorphlogopite crystal phase and this might tend to increase the activation energy .

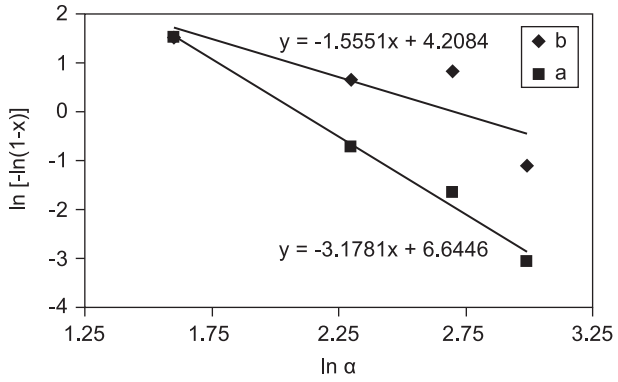

Figure 5. Plot of ln[-ln(1-x)] vs. lnα for: a) A_0 at 1050 K, b) A_5 at 955 K.

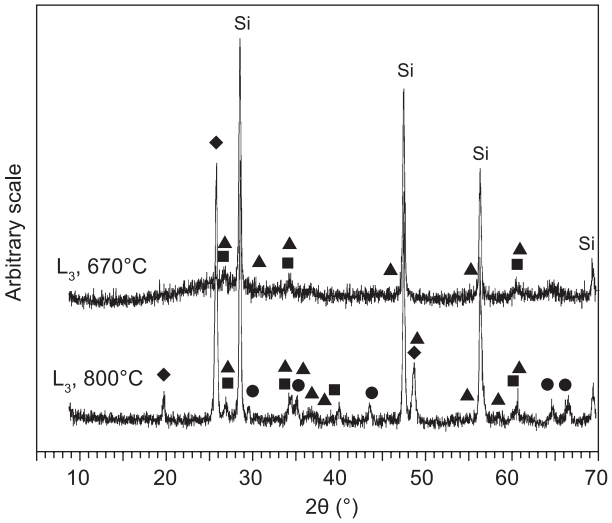

Figure 8. XRD patterns of A_3 sample heated at 670°C and 800°C for 2 h (■ - Phlogopite, ● - Potassium Titanicum Silicate, ♦ - b-Spodumene, ▲ - Chondrodite).

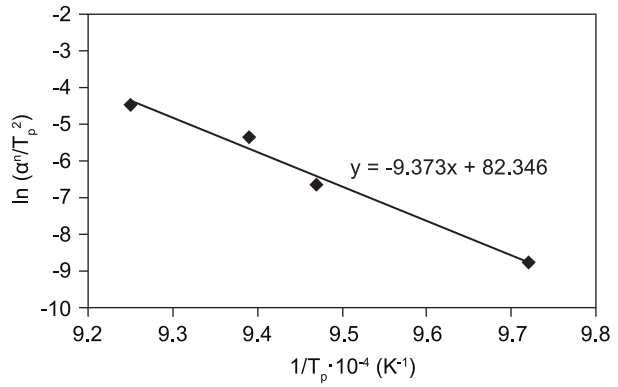

a)

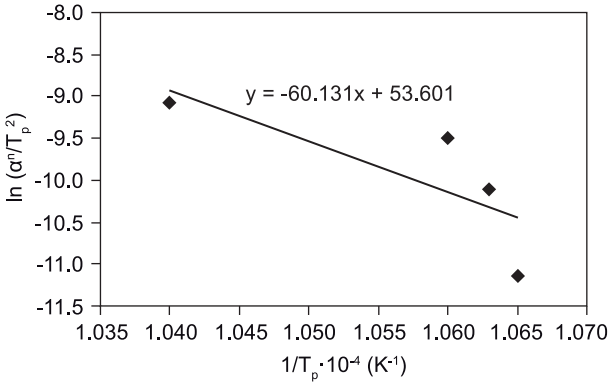

b)

Figure 6. The Matusita-Sakka plots of the: a) A_0, b) A_5.

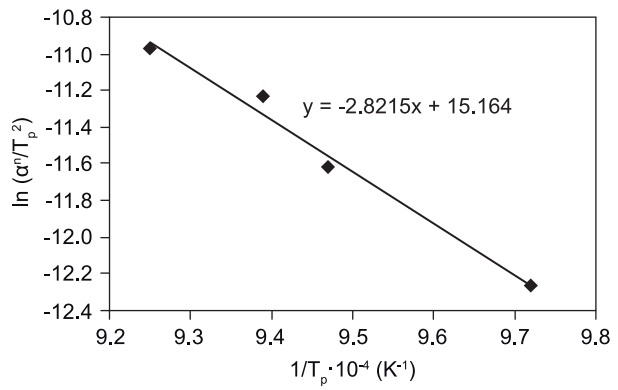

a)

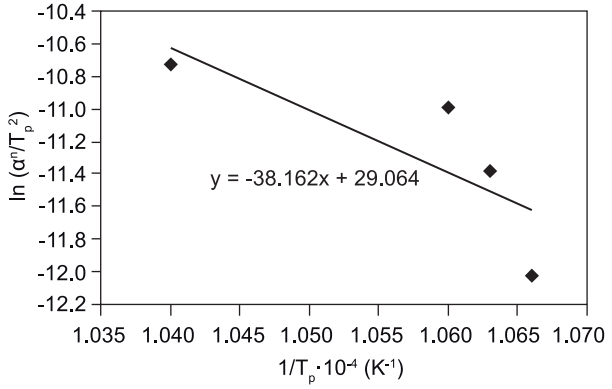

b)

Figure 7. The Matusita-Sakka plots of the: a) A_0, b) A_5.

The XRD patterns of all samples, annealed at the temperatures determined by DTA exothermic peak, show crystallization of potassium–mica and potassium titanium silicate phases in the A_0 sample that heat-treated at 775°C and 830°C. Whereas in the case of A_3 sample heat treatment was conducted at 670°C for 2h. Existence of chondrodite and potassium-mica phases with low intensity confirm that amount of these phases in this sample are relatively low. In this sample, with increasing temperature up to 800°C, potassium-mica, potassium titanium silicate and -spodumene phases were formed (Figure 8). It seems that in this sample, Li^+ ions prefer to precipitate as -spodumene phase and residual Li_2O remains in the glass matrix. Chondrodite and -spodumene phases have been formed in 670°C in A_5 sample. With increasing of temperature up to 725°C, the relative intensity of these two phases were increased. At 830°C, the relative intensity of chondrodite phase was decreased and on the contrary,-spodumene phase content was increased.

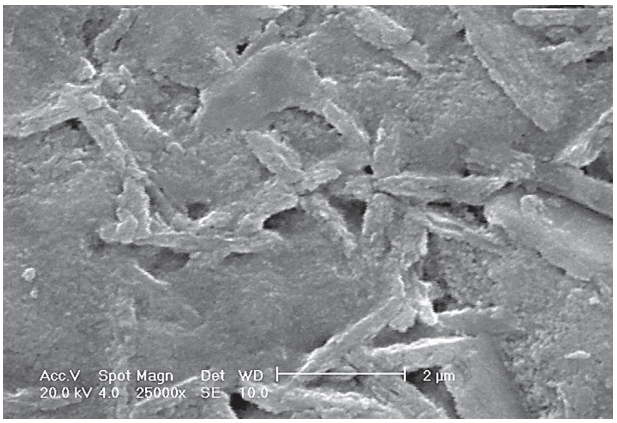

a)

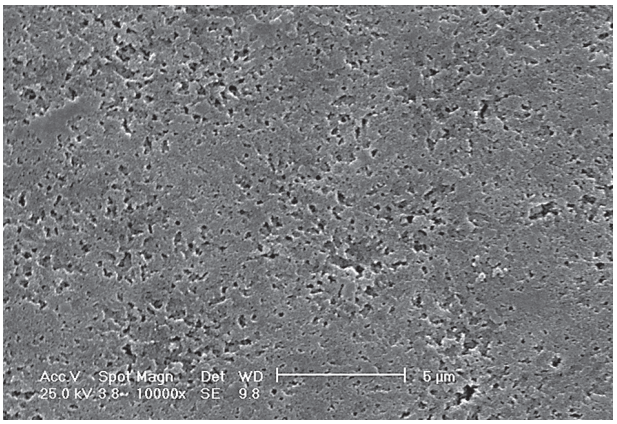

b)

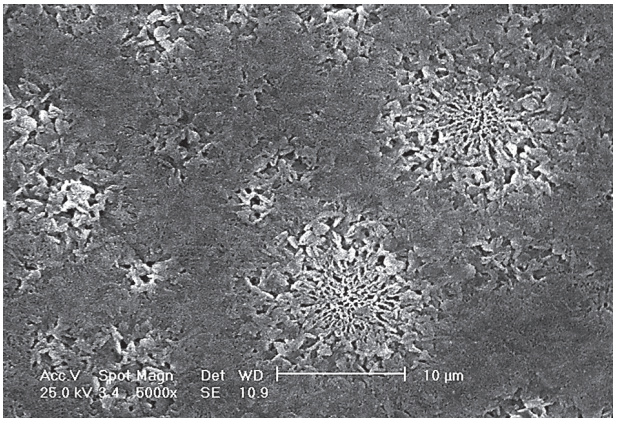

c)

Figure 9. SEM micrographs of: a) A_0 after heat treatment at 830°C for 2 h, b) A_3 after heat treatment at 800°C for 2 h, c) A_5 after heat treatment at 725°C.

Figure 9 shows the microstructure of different samples. In the case of A_0 specimen, low fraction of plate-like mica crystals were observed. In the A_3 and A_5 samples; a spatial orientation in the arrangement of crystals were observed. This microstructure is generally observed in samples having a low nucleation density; as it has been mentioned by others [17,18].

Machinability of the samples was not satisfactory. It seems to us that low machinability of the investigated samples is affected by a small amount of machinable mica phase, no interlocked structure and more content of glassy phase in the system. It seems that addition more of Li_2O to the base glass weakens machinability.

CONCLUSION

Crystallization kinetics of fluorphlogopite glass-ceramic were studied by DTA, XRD and SEM. DTA scans exhibited on well defined crystallization exotherm, which was formed by the overlapping of two exothermic crystallization curves. The activation energy of crystallization for the formation of first crystalline phase and Avrami parameter, (n) were obtained to be 246 kJ/mol and 3.17, respectively. These Avrami parameter corresponds to the bulk crystallizations. Substitution of Li_2O for K_2O in the samples changed the temperatures and sharpness of the crystallization peak. Activation energies for crystallization of first crystalline phase in sample with Li_2O was 322 KJ/mol. Avrami parameter, (n) was 1.55 corresponding to the bulk crystallization.

References

1. Alizadeh P., Marghussian V.K.: J. Eur. Ceram. Soc. *20*, 775 (2000).
2. Baik D.S., No K.S., Chun J.S., Cho H.Y.: J. Mat. Proc.Tech. *67*, 50 (1997).
3. Taruta S., Mukoyama K., Suzuki S.S., Kitajima K., Takusayawa N.: J. Non–Cryst. Solids *296*, 201 (2001).
4. Henry J., Hill R.G.: J.Non –Cryst. Solids *319*, 1 (2003).
5. Davis J.B., Marshall D.B.: J. Am . Ceram. Soc. *81*, 2169 (1998).

6. Greene K., Promeroy M.J., Hampshire S. Hill R.: J. Non-Cryst. Solids *325*, 193 (2005).
7. Tatura S., Watanabe K., Kitajima K., Takusagawa N.: J. Non-Cryst. Solids *321*, 96 (2003).
8. Radonjic L., Nikolic L.: J. Eur. Ceram. Soc. *7*, 11 (1991).
9. Trauta S., Ichinose T., Yamaguchi T., Kitajima K.: J. Non-Cryst. Solids *352*, 5556 (2006).
10. Taruta S., Suzuki M., Yamakami T., Yamaguchi T., Kitajima K.: J. Non-Cryst. Solids *354*, 848 (2008).
11. Wang P., Yu I., Xiao H., Cheng Y., Lian S.: Ceram. Int. *35*, 2633 (2009).
12. Arora A., Shaaban E.R., Singh K., Pandey O.P.: J. Non–Cryst. Solids *354*, 3944 (2008).
13. Erol M., Kuchukbayrak S., Ersoy-Mericboyu A.: J. Non–Cryst. Solids *355*, 569 (2009).
14. Matusita K., Sakka S.: J. Non-Cryst. Solids. *38&39*, 741 (1980).
15. EKissinger H.: J. Res. Nat. Bur. Stand. *57*, 217 (1956).
16. Birkan A., Yavuz H.: Materials Letters *57*, 4382 (2003).
17. Moisescu C., Jana C., Russel C.: J. Non-Cryst. Solids *248*, 169 (1999).
18. Thomas H., Habelitz S.: J.Crystal Growth *192*, 185 (1998).